# Laser-induced electronic processes on GaP (110) surfaces: Particle emission and ablation initiated by defects

Ken Hattori,* Akiko Okano, Yasuo Nakai, and Noriaki Itoh
*Department of Physics, Faculty of Science, Nagoya University, Furocho, Nagoya 464-01, Japan*
(Received 7 October 1991)

We have carried out high-sensitivity measurements of $Ga^0$ emission from the GaP (110) surface by laser pulses of photon energies above the indirect-band-gap energy $E_G$ (range I), below $E_G$ but above the energy gap $E_{VS}$ between the valence band and the unoccupied surface band (range II), and below $E_{VS}$ (range III). Below the ablation threshold, we find that laser pulses of energy ranges II and III induce particle emission, the yield of which is reduced as the laser shots are repeated on the same spot. The dependence of the yield on the number of shots shows rapidly ($A$) and slowly ($S$) decreasing components. The $A$ component is found to be enhanced by $Ar^+$ bombardment and reduced by subsequent annealing. Measurements of the dependence of the pulse width show that the yield is scaled by the fluence for the $A$ component. The yields for both $A$ and $S$ components are superlinear functions of fluence, exhibiting apparent threshold laser fluences. The threshold laser fluence for the $A$ component is found to be smaller than that for the $S$ component. The yield-fluence relations can also be fitted to power functions: The power index for the $A$ component is 2–3 and, for the $S$ component, 4–6. These components are not induced by photons in energy range I. Above the ablation threshold the yield on the same spot is found to increase by repeating laser pulses. Nearly the same ablation threshold fluence was observed for photons in energy ranges I and II, while the ablation threshold is scattered for photons in energy range III. The results are interpreted in terms of a breaking of the bonds of loosely bound atoms near defects on surfaces by multiple electron-hole localization. Three types of defects are differentiated: adatom type, kink type on steps, and vacancy type. The $A$ and $S$ components are ascribed to be initiated by the adatom- and kink-type defects, respectively, and the laser ablation is ascribed to be initiated by vacancies. A model of localization is suggested.

## I. INTRODUCTION

Recently, laser-induced processes on surfaces of solids including laser annealing,[1] photochemical etching,[2] and laser damage,[3,4] have been topics of general interest. Some of these processes have been interpreted in terms of temperature effects. Rise in temperature is inevitable for intense laser beams of energies above the band-gap energy; most of the energy is absorbed by the surface layers. However, it is known that purely electronic particle emission occurs from alkali halides,[5] silver halides,[6] frozen gases,[7] and alkaline-earth fluorides,[3] by excitation with weak photon beams of energies above the band-gap energy. For semiconductors[8–11] and ionic oxides,[12,13] it has been shown recently that intense laser beams of subgap energies can induce particle emission. Maxwell distributions of ejected particles with characteristic temperatures much lower than the melting points[8,10] and low vibrational frequency of emitted molecular species[12] have been regarded as evidence for nonthermal nature of the processes.

Menzel and Gomer[14] and Readhead[15] (MGR) have suggested that desorption of adsorbates by excitation of valence electrons arises from excitation to an antibonding-type adiabatic potential-energy surface (APES). The MGR mechanism has been primarily applied to the desorption of adsorbates, but it has been suggested that an antibonding APES leading to emission of a halogen atom is formed in the proximity of a self-trapped exciton (STE) near the surface of alkali halides.[16,17] Thus, the MGR model can explain particle emission from solids in which excitons are self-trapped. In these solids the yield is proportional to the number of self-trapped excitons generated, and the emission is evidenced by a low-intensity band-to-band transition.[18] Knotek and Feibelman[19] (KF) have proposed that multihole localization at an anion site on a surface that originated from interatomic core-hole Auger decay induces Coulomb instability and, consequently, particle emission. Both MGR and KF mechanisms can explain the processes of particle emission, of which the yield is proportional to the number of transitions.

The laser-induced particle emission from semiconductors[8,9] and ionic oxides[12,13] is known to be a nonlinear process: the yield is proportional to a superlinear function of the fluence of the laser pulse. Since low-intensity band-to-band transitions cannot induce particle emission in these materials,[20] multiphoton absorption cannot be the cause of the particle emission.[21] Thus, even if the origin of the process is electronic, neither the MGR nor the KF mechanism can be used to explain the results. Wu suggested a mechanism of localization of two holes on a defect through Auger recombination processes.[22] Itoh and Nakayama[23] have suggested that dense valence-electron excitation leads to localization of two holes at an atom on the surface by negative-$U$ interaction, originally suggested by Anderson for defect states in the bulk of solids.[24] Here it is assumed that localization of two holes

 

on a bond, by virtue of electron-lattice interaction, leads to a bond breaking. It has been argued that two-hole localization by the negative-$U$ interaction occurs because of the screening of Coulomb repulsion between holes under an electron-hole ($e$-$h$) plasma.[23] Alternatively, Sumi pointed out that the occupancy of the low-lying states of the valence band increases the Fermi energy for holes and, hence, enhances the tunneling to form the two-hole states.[25]

The present authors have recently reported evidence for defect-initiated emission of $Ga^0$ from GaP (110) (Ref. 26) and $(\bar{1}\,\bar{1}\,\bar{1})$ (Ref. 21) surfaces. They employed well-characterized cleaned surfaces and a high-sensitivity detection technique. It was shown that repeated irradiation on the same spot of the surface induces the change in the yield, $Y$, and that the relation ($Y$-$n$ relation) between $Y$ and the number, $n$, of shots, as well as the $Y$-fluence ($Y$-$\phi$) relation, yield useful information on the change of the surface morphology. The results were interpreted in terms of the interaction of the $e$-$h$ pairs with various types of defects on the surfaces.

It is the purpose of the present paper to report the response to several types of excitation of surfaces annealed to several stages after $Ar^+$ bombardment, observed through $Ga^0$ emission. Some of the important results reported elsewhere are described here in order to make the description complete. According to inverse-photoemission measurements, the GaP (110) surface has unoccupied surface states about 0.3 eV below the bottom of the bulk conduction band.[27] Thus, the electrons in the valence band or the occupied surface state located 0.06 eV below the top of the valence band[28] can be excited to the unoccupied surface states by photons above the energy $E_{VS}$ (1.53 eV), the separation between the valence band and the surface state (see Fig. 1). In this case we expect that the $e$-$h$ pairs, the motion of which is confined to two-dimensional (2D) surfaces, are produced, while photons above the indirect band gap $E_G$ (2.26 eV) produce three-dimensional (3D) $e$-$h$ pairs. In the present work we used three wavelength ranges: one (range I) above $E_G$, a second (range II) slightly below $E_G$, and a third (range III) much lower than $E_G$. We consider energy range II to lie between $E_{VS}$ and $E_G$ and energy range III to lie below $E_{VS}$.[28,29] We found that the particle emission initiated by defects lying on the surface is induced by photons of ranges II and III, while laser ablation is induced by photons of all ranges.

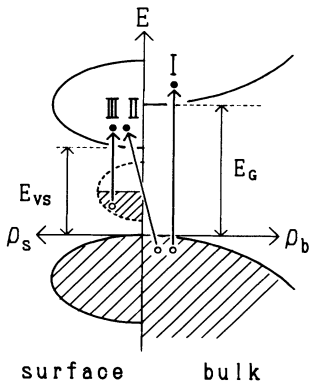


FIG. 1. Schematic diagram of the density, $\rho_b$, of the states for bulk GaP and that, $\rho_s$, for the GaP (110) surface. $E_G$ (=2.26 eV) is the bulk indirect-band-gap energy and $E_{VS}$ (=1.53 eV; see Ref. 28) the energy between the valence-band maximum and the minimum of the unoccupied surface states. Dashed line illustrates surface defect states located in the band gap. Arrows labeled I, II, and III indicate the plausible transitions induced by photons of energy range I (larger than $E_G$), II (between $E_G$ and $E_{VS}$), and III (smaller than $E_{VS}$), respectively. Transition II may include the transition from the occupied surface state, which is located 0.06 eV below the top of the valence band (see text).

## II. EXPERIMENTAL PROCEDURE

The experimental procedures used in the present work are almost the same as those described elsewhere.[26] The specimens were $n$-type ($S$-doped) GaP single crystals, measuring $10\times15\times2$ mm$^3$, the wide faces of which were parallel to the (110) plane. The surface, which was polished mechanically and etched chemically, was cleaned in an ultrahigh-vacuum (UHV) chamber by 0.5-keV $Ar^+$-ion bombardment at a beam current of 2–3 $\mu$A for 30 min and annealed thermally at 500–600 °C for several time intervals of not more than 10 min. We refer to a surface annealed for 10 min as a well-annealed surface; surfaces annealed for intermediate times are referred to as partially annealed surfaces. After cleaning, the (110) surface showed a clear (1×1) low-energy electron-diffraction (LEED) pattern, as observed by Bommel and Crombeen,[30] and indicated no Auger signals due to surface contamination.

A schematic diagram of the experimental setup is shown in Fig. 2. The "pump" laser beams for irradiation were either 28-ns pulse-laser beams generated by an excimer-pumped dye laser (Lambda Physik, EMG203MSC and FL3002) of wavelengths of 540, 600, 870, and 920 nm, or 0.6-$\mu$s pulse beams generated by a Xe-flash-lamp-pumped dye laser (Phase-R, DL-2100A2) of a center wavelength of 613 nm. In the present study

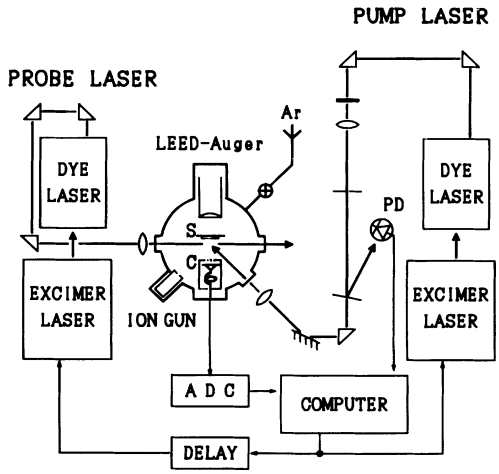


FIG. 2. Experimental setup for measurements of high-sensitivity laser-induced particle emission.

we used mostly 28-ns laser pulses, except for investigating the effects of the pulse width. The pump-laser beam was an incident on the specimen at an angle of 45° from the surface normal, and its spot size on the surface was about 0.5 mm in diameter. The power of laser pulses was monitored with a photodiode calibrated by a calorimeter. Because of a 10–20% error in the spot size measured by means of patterns on Polaroid® films, the absolute value of the laser fluence may include an error of about 30%. However, the relative values of the laser fluence in a series of experimental runs, carried out under the same laser conditions, can be compared with an accuracy of 5%. The frequency of the laser pulses was below 0.3 Hz.

Emitted $Ga^0$ neutral atoms were detected using the technique of resonance-ionization spectroscopy (RIS).[31] $Ga^0$ atoms emitted were ionized by 28-ns "probe" laser beams, which include fundamental and frequency-doubled beams, generated by a second excimer-pumped dye laser (Lambda Physik, EMG203MSC and FL3002) tuned at a wavelength of 574.82 nm. The frequency-doubled beam induces the $^2P_{1/2}$-$^2D_{3/2}$ transition of $Ga^0$ atoms, while the fundamental beam ionizes excited $Ga^0$ atoms. The probe beams, the diameter of which was about 1.0 mm, were triggered about 3.3 $\mu$s after each shot of the pump-laser pulses, and they passed parallel to the surface at a distance of 2.0 mm. $Ga^+$ ions were detected by a Channeltron, biased negatively and facing the surface, and the signals were stored in a microcomputer through an analog-to-digital converter. We evaluated the detection limit of $Ga^0$ atoms emitted by a laser pulse to be $10^{-7}$ monolayer (ML), taking the ionization efficiency and the geometrical factor into account. LEED and Auger-electron spectroscopy studies were made using a LEED-Auger spectrometer. Measurements of laser-damaged surfaces using scanning electron microscopy (SEM) and electron-probe microanalysis (EPMA) were made after exposing the specimen to air. The base vacuum pressure is less than $2\times10^{-8}$ Pa. All measurements were carried out at room temperature.

## III. RESULTS

We carried out measurements for surfaces—well annealed, partially annealed, $Ar^+$-ion bombarded, and laser damaged—using photons of energy ranges I, II, and III. We describe the results for photon-energy range II in subsections A–D, and those for energy ranges I and III in subsection E.

### A. Shot-number dependence

We measured the $Ga^0$ yield $Y$ from partially annealed GaP (110) surfaces induced by repeated irradiation with 28-ns laser pulses of a fixed laser fluence on the same spot. Figures 3(a) and 3(b) show typical $Y$-$n$ relations for a wavelength of 600 nm (2.07 eV), obtained at fluences of 1.0 and 1.2 J/cm$^2$, respectively. Almost no signal was detected for a fluence of 1.0 J/cm$^2$ in well-annealed specimens, as will be described later, while the $Y$-$n$ relation for a fluence of 1.2 J/cm$^2$ in well-annealed specimens was substantially the same as shown in Fig. 3(b). For each fluence, the counting of the number of laser shots was started on an unirradiated spot. The fluctuation of the fluence was about 5%. As shown in Fig. 3(a), $Y$ decreases with increasing $n$ at the initial state ($n < 100$), and reaches a nearly constant value, which decreases very slowly and lasts over 8000 shots. The semilogarithmic plots of the $Y$-$n$ relation are shown in the inset of Fig. 3(a): the function $Y(n)$ was fitted to the summation of two exponential functions of the form $Y_0\exp(-\beta n)$, with $Y_0=3.0$, $\beta=3.6\times10^{-2}$ and $Y_0=0.12$, $\beta=1\times10^{-4}$. We refer to the rapidly decreasing component as the $A$ component and the nearly constant component as the $S$ component. We evaluated the unity of the ordinate scale to be about $10^{-6}$ ML. The noise level of the detection was about 0.05. We found that the (1×1) LEED pattern obtained after 8000 shots of a fluence of 1.0 J/cm$^2$ was unchanged.

The $Y$-$n$ relation for $\phi=1.2$ J/cm$^2$ shows an increase

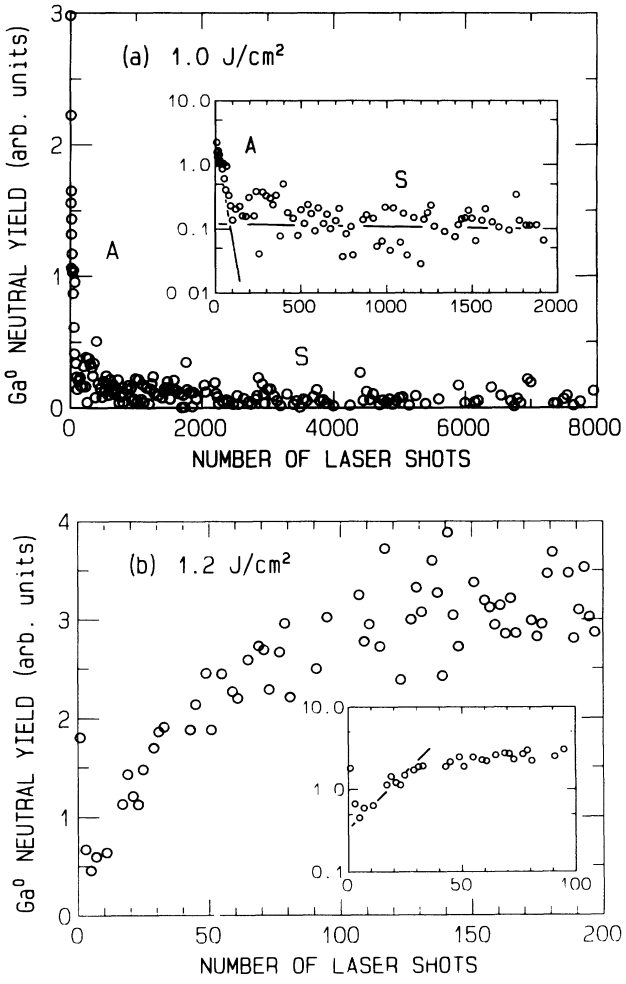


FIG. 3. Linear plots and semilogarithmic plots (inset) of $Ga^0$ yield induced by 600-nm laser beams from a partially annealed GaP (110) surface as a function of the number of laser shots, at fluences of (a) 1.0 J/cm$^2$ and (b) 1.2 J/cm$^2$. A new spot was exposed to the laser beam at the start of the experimental run for each fluence and the same spot was irradiated repeatedly. For 1.0 J/cm$^2$ the $Ga^0$ yield decreases rapidly ($A$ component) and becomes almost constant ($S$ component), while the yield increases by repeating pulses for 1.2 J/cm$^2$.

in $Y$ with increasing $n$ after an initial rapid decrease for a few pulses. The rapidly decreasing component is regarded as the $A$ component described above. The semilogarithmic plots of the $Y$-$n$ relation shown in the inset of Fig. 3(b) indicates that $Y(n)$ was fitted to $Y_0\exp(\beta n)$ with $\beta=6\times10^{-2}$ for $n<30$. We note a remarkable difference of the $Y$-$n$ relation by changing $\phi$ only by 20% across a critical laser fluence $\phi_D$, which we evaluate to be 1.1 J/cm$^2$. We also found that each spot of the (1×1) LEED pattern became weaker by repeated irradiation above $\phi_D$, while no change was observed by repeated irradiation below $\phi_D$. Laser ablation of the surface after a few hundred laser shots above $\phi_D$ was obviously seen by SEM. The [P]/[Ga] ratio detected by EPMA was 1.2 on the laser-ablation spot, and 2.1 on the well-annealed spot, indicating that irradiation above $\phi_D$ produces Ga-rich layers. Such modification of the surface stoichiometry has been observed in III-V-compound semiconductors after laser ablation by laser beams of energy range I.[32] Since disappearance of crystalline structure and change in stoichiometry are common features of laser ablation, we tentatively refer to $\phi_D$ as the ablation threshold.

### B. Fluence dependence

No Ga$^0$ emission is observed at low laser fluences, even for a partially annealed surface, but emission starts to be observed at a fluence above approximately $0.1\phi_D$. A typical $Y$-$\phi$ relation obtained at 600 nm on the same spot on a partially annealed surface by a step-by-step increase of the fluence is shown in Fig. 4(a). Evidently, the yield increases superlinearly with respect to $\phi$ above the threshold. The $Y$-$\phi$ relation obtained includes the effects of the reduction of $Y$ with repeating laser pulses as described before.

In order to obtain the $Y$-$\phi$ relation for specimens from which the $A$ component is eliminated by repeated irradiation, we carried out the following experiments, the results of which are shown in Fig. 4(b). First, we repeated irradiation of a new spot on the surface starting from a low fluence and obtained curve 1, which corresponds to the curve in Fig. 4(a). Next, we fixed the fluence at $\phi_2=0.85$ J/cm$^2$ and repeated the irradiation, and observed a decrease in $Y$, as indicated by the downward arrow labeled 2. When $Y$ became almost constant, we reduced $\phi$ step by step and obtained curve 3. Finally, we fixed the fluence at $\phi_4=1.3$ J/cm$^2$, above $\phi_D$, and repeated the irradiation, and observed an increase in $Y$, as indicated by the upward arrow labeled 4.

From Fig. 4(b) it is evident that there are two different threshold laser fluences below which no emission is practically observable. The threshold laser fluence $\phi_A$ for a new spot on the partially annealed surface is 0.07 J/cm$^2$. On the other hand, after the repeated irradiation at $\phi_2$, we observed the threshold laser fluence $\phi_S=0.5$ J/cm$^2$. Clearly, $\phi_A$ is the threshold for the $A$ component and, since the $A$ component is eliminated by repeated irradiation, we consider $\phi_S$ to be the threshold for the $S$ component.

In order to examine the degree of the superlinearity of the $Y$-$\phi$ relations, in Fig. 4(c) we made logarithmic plots of curves 1 and 3 of Fig. 4(b). Clearly, the $Y$-$\phi$ relations

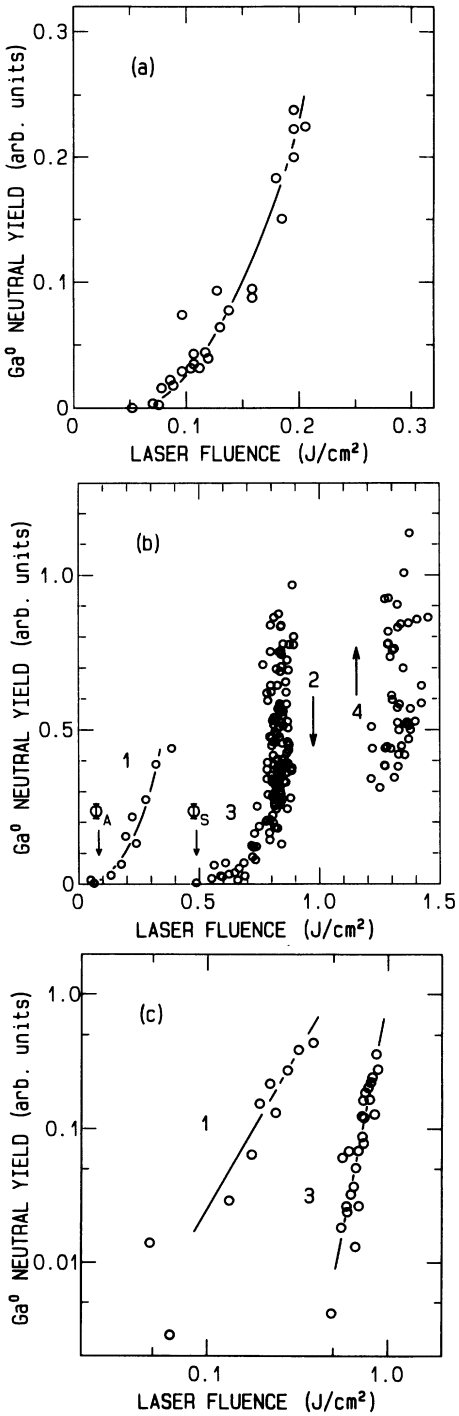


FIG. 4. Dependence of Ga$^0$ yield on 600-nm laser fluence for a partially annealed GaP (110) surface. (a) Typical result obtained on the same spot by increasing the fluence gradually starting from a new spot. (b) Results obtained on the same spot by sequential irradiation by varying the fluence as described below: Curve 1, the laser fluence was increased; curve 2, the laser fluence was kept constant at $\phi_2=0.85$ J/cm$^2$; curve 3, the laser fluence was decreased; and curve 4, the laser fluence was kept constant at $\phi_4=1.35$ J/cm$^2$. Arrows 2 and 4 show the direction of the change of the yield by the sequential irradiation. Fluences $\phi_A$ and $\phi_s$ indicate the threshold fluences for curves 1 and 3, respectively. (c) Logarithmic plots of curves 1 and 3 of (b), showing power indices 2.3 and 5.7, respectively.

can be expressed as $Y \propto \phi^m$. The power indices for curves 1 and 3 are 2.3 and 5.7, respectively. As we describe later, we consider that the $Y$-$\phi$ relation should be represented by a power function and that the threshold laser fluences are simply an indication of highly superlinear character, but not of any critical behavior.

### C. Effects of surface defects

Below the ablation threshold, we observed the change in the yield of particle emission caused by repeating laser shots. Since no evolution of surface damage is observed in this range of laser fluences, the gradual change in the yield should be ascribed to the modification of surface morphology not relevant to laser ablation. Most plausible causes of such modification are defect-related processes: elimination of defects on surfaces and the change of the defect structures on surfaces.

In order to obtain evidence for the contribution of defects to particle emission, we measured the effects of $Ar^+$ bombardment and of subsequent annealing on the $Y$-$n$ and $Y$-$\phi$ relations. Figure 5 shows the effects of $Ar^+$ bombardment on the $Y$-$n$ relation. In this experiment, we measured $Ga^0$ emission for 400 shots, starting on an unirradiated spot of a partially annealed surface with 600-nm laser pulses of a fixed fluence of 0.6 J/cm$^2$. Then the surface was bombarded with 0.5-keV $Ar^+$ ions for 30 min, and the measurement was continued on same spot of the specimen. As seen in the figure, a burst of the yield is induced by $Ar^+$ bombardment, although it is not seen if the specimen was not bombarded. Since the yield decreases with repeating pulses after $Ar^+$ bombardment, the burst can be regarded as the $A$ component.

Figure 6 shows the effects of thermal annealing after $Ar^+$ bombardment on the $Y$-$\phi$ relation measured with

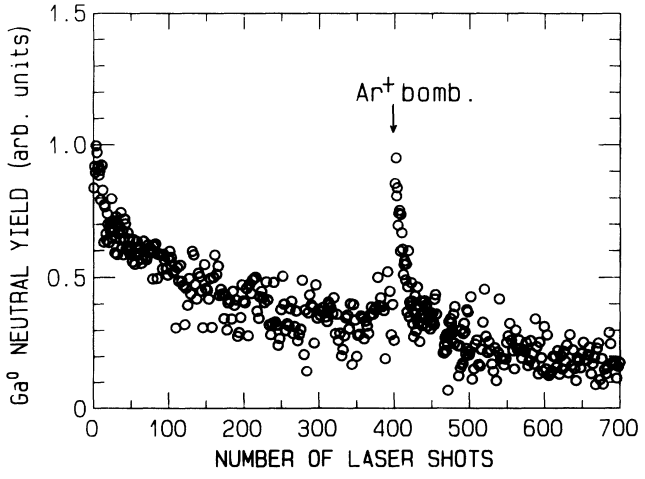


FIG. 5. Effect of $Ar^+$ bombardment on the dependence of $Ga^0$ yield on the number of laser shots for 600 nm, on the same spot of a partially annealed GaP (110) surface, obtained at a fluence of 0.6 J/cm$^2$. The abscissa is the number of shots on a new spot on the surface: The laser irradiation was paused at 400th shot, the surface bombarded with $Ar^+$ ions, and then the irradiation of the same spot was continued.

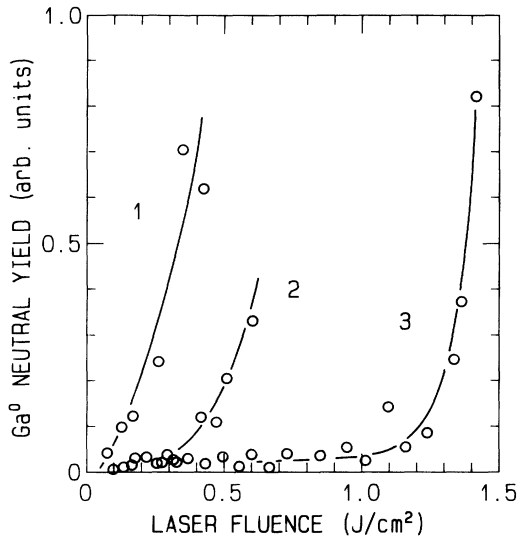


FIG. 6. Effect of thermal annealing after $Ar^+$ bombardment on the dependence of $Ga^0$ yield on the laser fluence for 600-nm photons. Curves 1, 2, and 3 were obtained starting from a low fluence on a new spot of the GaP (110) surface after $Ar^+$ bombardment, subsequent partial annealing, and full annealing, respectively. The values of the power indices of curves 1 and 2, when plotted on a double-logarithmic scale, are 1.7 and 3.3, respectively.

600-nm laser pulses. Each curve was obtained on a new spot after preparation by changing $\phi$ from the low-fluence side: curve 1 after bombardment with $Ar^+$ ions and curves 2 and 3 after annealing at 500–600 °C for 6 min (partially annealed) and for 10 min (well annealed), respectively. We made similar measurements on other spots after the same treatments, but results were substantially the same. It is clear that the emission yield at a given fluence decreases drastically as the surface is annealed after $Ar^+$ bombardment. After obtaining each curve, we repeated irradiation on the same spot at the fluence employed to obtain the last plot of the curve. The $Y$-$n$ relations obtained after curves 1 and 2 show decreases of $Y$ with increasing $n$; hence, we can regard curves 1 and 2 as the emission of $A$ components. The $Y$-$n$ relation after curve 3 showed an increase. On the same specimen the $Y$-$n$ relation at 1.1 J/cm$^2$ did not show any increase. Thus, the threshold laser fluence in this case lies between 1.1 and 1.4 J/cm$^2$.[33] We observed that, after eliminating the $A$ component by irradiation of a partially annealed surface, the $Y$-$\phi$ relation obtained by a step-by-step increase of the fluence leads to a curve that is almost the same as curve 3 of Fig. 6. Thus, it appears that the well-annealed and partially annealed surfaces have almost the same ablation threshold. The ablation threshold after repeated irradiation of $Ar^+$-bombarded surfaces, obtained similarly, appears to be slightly smaller than that of a well-annealed surface.

In order to see the correlation between the characteristics of laser-induced particle emission and other properties of surfaces, in Table I we show the values of the power indices for the $Y$-$\phi$ relation of the $A$ component,

TABLE I. Value of the power index $m$ for the $Y$-$\phi$ relation obtained at the initial stage of laser irradiation ($A$ component), the ratio of the [P]/[Ga] Auger signal ratio, and the LEED pattern of GaP (110) surfaces that were $Ar^+$ bombarded and subsequently annealed.

| Annealing time (min) | $m$ | [P]/[Ga] | LEED |
|---|---|---|---|
| 0 | 1.7 | 2.4 | no pattern |
| 3 | 3.3 | 4.2 | (1×1) |
| 6 | 3.3 | 4.2 | (1×1) |
| 10 | | 4.2 | (1×1) |

the ratio of the Auger P (120 eV) and Ga (52 eV) lines, and the features of the LEED patterns, for surfaces at several stages of annealing after $Ar^+$ bombardment. It is clear that the values of the power index and the [P]/[Ga] Auger-signal ratio increase with annealing up to 3 min and do not change afterward. The dependence of the [P]/[Ga] ratio on annealing is consistent with the result of Bommel and Crombeen.[30] After annealing for more than 3 min, a clear (1×1) LEED pattern was observed. Clearly, there is a remarkable difference in the magnitude of the $A$ component obtained at different annealing stages for which no distinction can be made by means of Auger and LEED techniques.

Figure 7 shows the $Y$-$\phi$ relations measured with 600-nm laser pulses on a well-annealed (curve 1) and a laser-damaged (curve 2) surface. In this experiment, we irradiated a new spot of the well-annealed surface, starting from a low fluence to obtain curve 1, and curve 2 was obtained on the same spot starting from a low fluence after curve 1 was taken. Curve 1 exhibits a power function with an index 15. It is clear that the emission efficiency

TABLE II. Threshold, $\phi_A$, for the $A$ component, and ablation threshold, $\phi_D$, obtained for laser pulses of widths of 28 ns and 0.6 $\mu$s on partially annealed surfaces. $F_A$ and $F_D$ are the calculated threshold fluxes from $\phi_A$ and $\phi_D$, respectively.

| Pulse width | $\phi_A$ (J/cm$^2$) | $F_A$ (J/cm$^2$ s) | $\phi_D$ (J/cm$^2$) | $F_D$ (J/cm$^2$ s) |
|---|---|---|---|---|
| 28 ns | 0.07 | $2.5\times10^6$ | 1.1 | $3.9\times10^7$ |
| 0.6 $\mu$s | 0.2 | $3.3\times10^5$ | 15 | $2.5\times10^7$ |

at a given fluence above 0.5 J/cm$^2$ is enhanced remarkably by laser damage. For curve 2, we observed an increase of $Y$, when irradiation is repeated at the highest laser fluence in the plots, indicating that enhanced yield is not due to the $A$ component. It appears that the laser-damaged surface is converted in such a way that further ablation proceeds at much lower fluences.

### D. Pulse-width dependence

One of the important questions for a superlinear process induced by pulse-laser beams is whether the fluence or the flux is the rate-determining quantity. We carried out measurements of the threshold for the $A$ component and the laser-ablation threshold on partially annealed surfaces, using laser beams of pulse widths of 0.6 $\mu$s and 28 ns. Although the wavelength (600 nm) of the 28-ns laser pulses is slightly different from that (613 nm) of the 0.6-$\mu$s pulses, we confirmed that 600- and 620-nm laser pulses 28 ns wide give almost the same threshold.[34] Table II shows the values of the threshold $\phi_A$ for the $A$ component and the ablation threshold $\phi_D$. It also shows values of the calculated fluxes $F_A$ and $F_D$ corresponding to $\phi_A$ and $\phi_D$, respectively, obtained assuming that the laser pulses are rectangular. We note that $F_D$ for 0.6-$\mu$s pulses is nearly the same as that for 28-ns pulses, while $\phi_A$ for 0.6-$\mu$s pulses is nearly the same as that for 28-ns

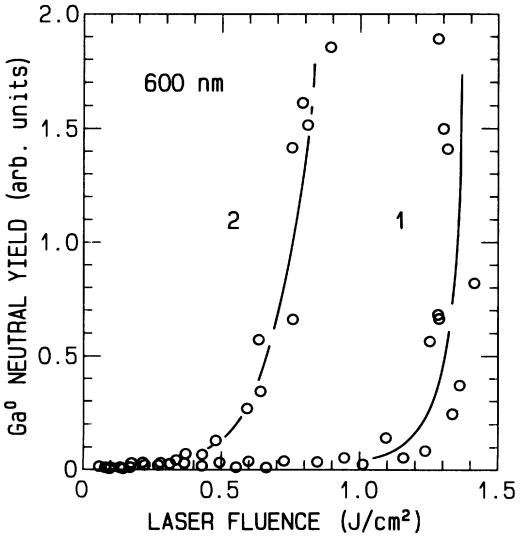


FIG. 7. $Ga^0$ yield as a function of fluence for irradiation with 600-nm laser pulses on GaP (110) surfaces, well annealed (curve 1) and laser damaged (curve 2). The value of the power index of curve 1 is about 15.

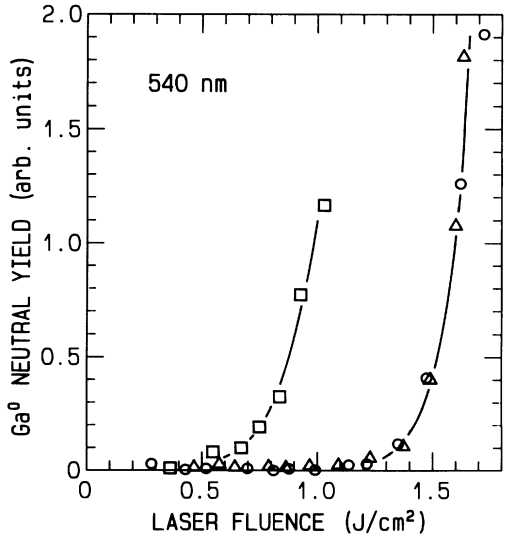


FIG. 8. $Ga^0$ yield as a function of fluence for irradiation with 540-nm laser pulses on GaP (110) surfaces, well annealed (circles), $Ar^+$ bombarded (triangles), and laser damaged (squares).

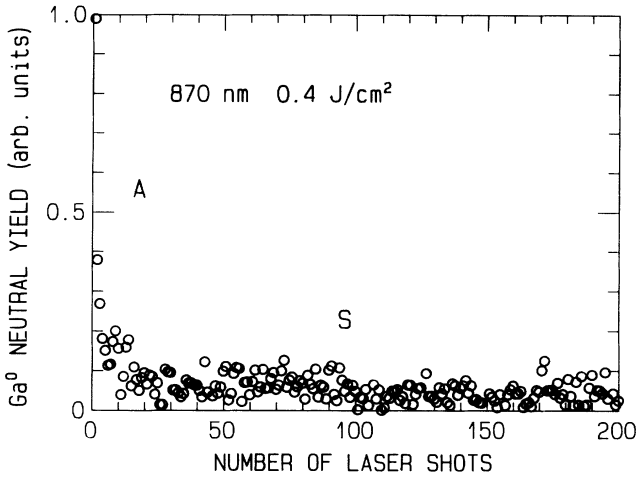


FIG. 9. $Ga^0$ yield as a function of the number of shots, obtained by repeating laser pulses of 870-nm photons at a fluence of 0.4 J/cm$^2$ on a new spot of a partially annealed GaP (110) surface.

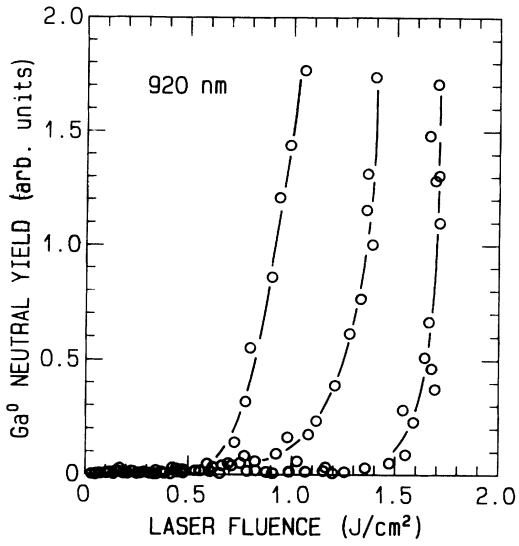


FIG. 10. $Ga^0$ yield as a function of laser fluence for a well-annealed GaP (110) surface measured with 920-nm photons. Each curve was obtained on a new spot starting from a low fluence.

pulses. Apparently, the ablation threshold is scaled by the flux, while the threshold for the $A$ component is scaled by the fluence.

### E. Comparison of the results for photon-energy ranges I, II, and III

All measurements described above were performed using photon energies of range II. In order to see whether the effects described above are due to the transition of the electron in the valence band to the unoccupied surface state, we measured $Y$-$n$ and $Y$-$\phi$ relations for photon-energy range I, 540 nm (2.30 eV), and range III, 870 nm (1.43 eV) and 920 nm (1.35 eV).

Figure 8 shows the $Y$-$\phi$ relations measured at 540 nm on the well-annealed (circles), $Ar^+$-bombarded (triangles), and laser-damaged (squares) surfaces. No yield is observed at fluences below $\phi_D = 1.2$ J/cm$^2$ on both the well-annealed and $Ar^+$-bombarded surfaces. Repeated irradiation at the highest fluence after obtaining each curve increased the yield, indicating that the increase of the yield for each curve represents laser ablation. Clearly, the ablation threshold at 540 nm does not differ remarkably from that at 600 nm. Similarly to 600-nm laser pulses, the ablation occurs at much lower fluences after the well-annealed surface is damaged by laser irradiation above the ablation threshold. We note that there was no indication of emission of the $A$ and $S$ components at 540 nm, as there was at 600 nm. Thus, clearly the $A$ and $S$ components are absent for irradiation with photons causing the band-to-band transition.

TABLE III. Summary of the observation of the $A$ and $S$ components and laser ablation on differently prepared surfaces for photons of wavelengths of 540, 600, and 920 nm. The symbol ○ indicates that $A$ or $S$ components are observed and $X'$ indicates that they are not observed.

| Wavelength (nm) | Preparation | $A$ | $S$ | Laser ablation |
|---|---|---|---|---|
| 540 | well annealed | × | × | threshold nonscattered |
| | partially annealed | × | × | |
| | $Ar^+$ bombarded | × | × | threshold reduced slightly |
| | laser damaged | | | threshold reduced |
| 600 | well annealed | × | × | threshold nonscattered |
| | partially annealed | ○ | ○ | |
| | $Ar^+$ bombarded | ○ | ○ | threshold reduced slightly |
| | laser damaged | × | × | threshold reduced |
| 920 | well annealed | × | × | threshold scattered |
| | partially annealed | ○ | ○ | |
| | $Ar^+$ bombarded | ○ | ○ | |
| | laser damaged | | | threshold reduced |

The dependence of $Ga^0$ yield from a partially annealed surface on the number of shots for 870-nm laser pulses of fluence 0.4 J/cm$^2$ is shown in Fig. 9. Evidently, the $A$ and $S$ components are observed for irradiation at 870 nm. We measured the $Y$-$\phi$ relations with photons of 920 nm on the well-annealed surface, for which 600-nm laser pulses do not produce the $A$ and $S$ components. Typical results are shown in Fig. 10, in which each curve represents emission from a new surface spot, obtained from the low-fluence side. Repeated irradiation at the highest fluence for each spot shows an increase in the yield. Thus, the increase of the yield is due to laser ablation. We note that the ablation thresholds on the different spots are not the same. It follows that the ablation threshold at 920 nm exhibits a broad distribution, contrary to that at 600 and 540 nm.

Table III summarizes the features of the $A$ and $S$ components and of laser ablation observed for wavelengths of three different ranges on the well-annealed, partially annealed, $Ar^+$-bombarded, and laser-damaged surfaces. The $A$ and $S$ components do not exist for excitation above $E_G$, while the excitations above $E_G$ and between $E_G$ and $E_{VS}$ behave similarly as far as the laser ablation is concerned.

## IV. DISCUSSION

First, we point out that the particle emissions designated as the $A$ and $S$ components originate from electronic excitation and not from heating. Indeed, we found that these emission processes are more efficient for photons of subgap energies. The absence of the photon-energy dependence of the laser-ablation threshold near the indirect-band-gap energy suggests that the laser ablation is also of nonthermal origin. We discuss this point later.

Another important feature of the present experimental results is that we have observed particle emission initiated by defects. In order that a particle is emitted from a defect site, the bond for an atom near the defect site should be broken as a result of electronic transition. Because of the superlinear dependence on the laser fluence, we presume that localization of multiholes on the defect site may weaken the bond and eventually lead to particle emission. Another remarkable feature of the present investigation is that $Ga^0$ particle emission depends strongly on the type of excitation: we used three types of excitation using three different ranges—I, II, and III—of photon energy. We presume that range-I photons produce exclusively 3D $e$-$h$ pairs; those of range II, 2D $e$-$h$ pairs near the surface; and those of range III, defect-excited states.

In this section we first discuss the phenomenology of the laser-induced particle emission, and then the microscopic mechanism.

### A. Types of defects initiating particle emission

Experimental results described in the preceding section clearly indicate that the $A$ component in the $Y$-$n$ relation is due to particle emission initiated by defects on the surface. First, the yield of Ga atoms is diminished by repeating laser pulses at a fixed fluence below the ablation threshold [Fig. 3(a)], where no change occurs in the LEED pattern. Second, the $A$ component is enhanced by $Ar^+$ bombardment (Fig. 5), which is known to generate surface defects. Third, the emission efficiency of the $A$ component in the $Y$-$\phi$ relation decreases with thermal annealing (Fig. 6). Since the emission yield diminishes rapidly as laser pulses are repeated, it appears that, after elimination of the defects responsible for the $A$ component, the surface becomes more resistive to laser beams. We refer to the surface defects causing the $A$ component as $A$-type defects.

We also ascribe the $S$ component to emission initiated by surface defects, although not as conclusively as the $A$ component. First, its yield decreases, not as significantly as the $A$ component, by repeating laser shots. Moreover, the $S$ component is not observed for well-annealed surfaces (curve 3 in Fig. 6), while it is observed for partially annealed surfaces [Fig. 3(a)]. We refer to the surface defects causing the $S$ component as $S$-type defects.

For any laser-induced emission of particles initiated by defects, the number, $dN_E(n)/dn$, of atoms emitted by the $n$th shot of laser pulses may be proportional to the concentration, $N_D(n)$, of weakly bonded atoms around defects (described as defect atoms[35]) remaining on the surface between the $(n-1)$st and $n$th shots,

$$\frac{dN_E(n)}{dn}=gN_D(n)\ , \tag{1}$$

where $g$ is the probability of a defect atom being emitted during a pulse. The experimental yield, $Y(n)$, per pulse is the summation of $dN_E(n)/dn$ arising from several types of defects: $Y(n)=\sum_i g_i N_D^{(i)}(n)$, where $g_i$ is the probability of a defect atom of the $i$th type to be emitted and $N_D^{(i)}(n)$ is their concentration.

In obtaining the dependence of $N_D$ on $n$, we consider three types of defects, as shown in Fig. 11: adatoms, kink sites of steps, and vacancies. Evidently, emission of an adatom restores the perfect lattice. It follows that

$$dN_E(n)=-dN_D(n)\ ,$$

and hence (2)

$$\frac{dN_E(n)}{dn}=gN_D(0)\exp(-gn)\ .$$

If emission is initiated by a kink site, removal of an atom transfers the defect atom to a nearest-neighbor site, keeping the structure of the defect unchanged, until the kink site interacts with another defect. Here we obtain

$$dN_E(n)\gg dN_D(n)\sim 0\ ,$$

and hence (3)

$$\frac{dN_E(n)}{dn}\sim \text{const}\ .$$

If an atom is ejected from one of the nearest sites around a vacancy, a divacancy is formed. Ejection of another atom from the divacancy creates a trivacancy, and so forth. Thus, a vacancy can be a nucleus for a vacancy cluster, which evolves by repeating the process of "vacancy"-initiated particle emission. When the size of a

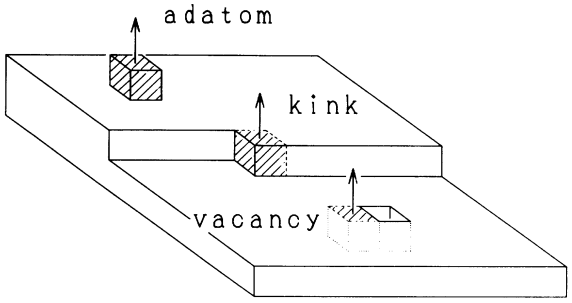


FIG. 11. Model of surface defects that initiate laser-induced particle emission. Three types of defects are considered: an adatom-type defect that is eliminated, a kink-type defect simply transferred to a neighboring site, and a vacancy-type defect evolving into a vacancy cluster, after particle emissions.

vacancy cluster is small, we expect that emission of an atom results in an increase of a defect atom. Thus, we obtain

$$dN_E(n)=dN_D(n)\ ,$$

and hence (4)

$$\frac{dN_E(n)}{dn}=gN_D(0)\exp(gn)\ .$$

If the size of a vacancy cluster increases, the increase in the yield with $n$ may be much slower.[36]

The $A$-type defects that give rise to the $A$ component may be ascribed to the adatoms. Using numerical values for the $A$ component and Eq. (2), we obtained the concentration, $N_D(0)$, of the $A$-type defects, $Y_0/\beta\sim 8\times 10^{-5}$ (ML). Although no other information on the adatoms on surface is yet available, we presume that the partially annealed surface includes adatoms of this amount. The $A$-type defects are not necessarily all adatoms; any defect, from which removal of a $Ga^0$ atoms makes it more resistive against laser-induced $Ga^0$ emission, satisfies the condition used in obtaining Eq. (2).

The $S$ component can also be ascribed to adatom-type defects. We have obtained $N_D(0)=Y_0/\beta=1.2\times 10^{-3}$ (ML) using Eq. (2). Here, we should assume that the $S$ component arises from the defects, which are more resistive (small $g$) to laser beams, but more numerous than the $A$ component. Another way of interpreting the $S$ component is that it arises from the kink sites of steps. The slow decrease in the yield [Fig. 3(a)] may be interpreted in terms of the loss of the kink sites due to interaction with other defects. At present we are unable to determine whether the $S$ component is due to adatom- or kink-type defects and unable to evaluate the defect concentration.

In this experiment we observed only the emission of $Ga^0$ atoms, but not P atoms, since the method of detecting $P^0$ at this level of sensitivity is not yet available. Thus, further explanation is needed on the definition of defect types $A$ and $S$. If a pair of Ga and P atoms is added on the surface, it also behaves as an $A$-type defect in any case where only the Ga atom is emitted or where both the Ga and P atoms are emitted by laser pulses. There are some other defects structures that may exhibit $A$-type behavior. For example, if emission of a P atom does not follow emission of a Ga atom from a kink site, then further emission of a Ga atom from the P-rich surface will not occur under the same irradiation conditions. Thus, the kinks having such a characteristic may be considered $A$-type defects. On the other hand, the $S$ component can be observed only when the emission of a Ga atom is followed by emission of a P atom, or vice versa, producing the same initial configuration. In order to reveal further details of the defect structures of each of the $A$- and $S$-type defects initiating the emission, it is useful to measure the P emission, but for the present argument measurements of Ga emission suffice.

### B. Superlinear dependence on the laser fluence for the $A$ and $S$ components

The superlinear dependence of the emission yield on laser fluence for the $A$ and $S$ components (Fig. 4) suggests that localization of a single hole is not sufficient to cause the emission of Ga atoms from the $A$- and $S$-type defects, but multihole localization is needed. We consider the value of the power index to be indicative of the multiplicity of hole localization on a defect needed for emission of a Ga atom. The power index $m$ shown in Table I indicates that approximately three holes are needed to break a bond of an $A$-type defect on partially annealed surfaces. As seen from Fig. 4(c), emission of a Ga atom from $S$-type defects needs localization of more holes.

Different values of the index $m$ for the $A$ component in Table I imply that the $A$ component is a composite. For instance, for the surface immediately after $Ar^+$ bombardment, $m=1.7$. It appears that the defects that give rise to the $m$ value are annealed by heat treatments for 3–6 min, leaving the defects showing higher $m$ values. It is likely that those $A$-type defects more strongly bonded on the surface show larger $m$ values. It follows that more holes are needed to break the bonds of defect atoms having higher thermal stability. Study of the pulse-width dependence indicates that the critical factor for bond breaking is the number of electronic transitions induced during a laser pulse. The mechanism of localization of holes during a pulse is discussed in Sec. IV F.

### C. Laser ablation

In the present work we found a sharp ablation threshold: the $Y$-$\phi$ relations for the $A$ and $S$ components exhibit power indices of 2–6, while that for the laser ablation is about 15, and a reduction of the laser fluence only by 20% from the laser fluence that gives rise to ablation does not induce laser ablation even by repeated irradiation (Fig. 3).[26] One of the significant results of the present investigation is that the ablation threshold can be clearly discernible by detecting only a very small number of atoms, of the order of $10^{-6}$ ML. It follows that the laser-ablation threshold does not represent the condition for a macroscopic change of surface layers under intense laser pulsation. It appears that, once the condition is satisfied, the surface is progressively damaged and finally exhibits a macroscopic change. We observed ablation on

well-annealed surfaces by 870- and 920-nm laser beams. Since photons of this energy can excite only the defect states, but cannot cause either the band-to-band transitions or the surface-state excitations, the results demonstrate that excitation of defects can initiate laser ablation.

In view of the above arguments, we suggest that laser ablation is initiated by a small number of defects on surfaces. The experimental results that the yield increases by repeating laser shots above the ablation threshold can be explained by Eq. (4), which assumes a vacancy as a source of particle emission. Thus, we consider that the condition for laser ablation is the same as that for breaking the bonds of atoms around vacancies. Irradiation with laser pulses, for which the condition is satisfied, causes evolution of vacancy clusters. As the evolution proceeds, the vacancies in the second layer start to be exposed to the laser beam. Using Eq. (4), surface damage can proceed both laterally and vertically to the surface.

The power index $m \sim 15$ for the laser ablation (Fig. 7), much larger than that of the $A$ and $S$ components, can be understood, if one takes into account the increase of the defect atoms around vacancy clusters within a laser pulse. We presume that the emission of a defect atom around a vacancy needs localization of $m'$ holes, and that $m'=4-6$ as for the $S$-type defects. The number of atoms emitted in $dt$ during a laser pulse is given by $dN_E(t)/dt=\sigma^{(m')}F^{m'}N_D(t)$, where $F$ is the flux and $\sigma^{(m')}$ is a constant. Using Eq. (4) the number of atoms emitted per pulse width $t_w$ is given by

$$N_E(t_w)-N_E(0)=N_D(0)[\exp(\sigma^{(m')}F^{m'}t_w)-1] . \quad (5)$$

Equation (5) gives a strong fluence dependence, since a power function is included in the exponent. Assuming that $m'=5$, it can give a power dependence with an index of 15 in a small flux interval near $\sigma^{(m')}F^{m'}t_w \sim 1$. According to Eq. (5), the ablation process is scaled by $\sigma^{(m')}F^{m'}t_w$. If $m'$ is substantially larger than 1, $F$ will be the dominant scaling factor, as observed experimentally (Table II). Further details of the model of laser ablation will be published elsewhere.[37]

### D. Dependence on types of excitation

As pointed out in Sec. III E, the $A$ and $S$ components are produced by excitation in photon-energy ranges II and III, but not in range I. The same conclusion has been drawn by Okano *et al.*[34] by measuring the temperature dependence of the emission yield by laser irradiation across the temperature at which the indirect-band-gap energy is coincident with the incident-photon energy. Emission of these components does not lead to any bulk destruction, but it is related to the change of the defect structures on the surface. Furthermore, the energy imparted to the lattice in a photoelectronic process is relatively small and, hence, only the atoms on surfaces are emitted. Thus, the results that the excitation in photon-energy ranges II and III can induce the $A$ and $S$ components substantiate the presumption that excitation by photons of range II and III involve the transitions on the surface.

The absence of the $A$ and $S$ components via excitation in range I, or via generating 3D $e$-$h$ pairs, implies either that excitation in range I does not create the 2D $e$-$h$ pairs or that the 2D $e$-$h$ pairs generated by photons of this energy range do not induce the $A$ and $S$ components. The 2D $e$-$h$ pairs may not be generated if the transition probability to the surface states existing near the conduction-band minimum is lower than that for lower photon energies. Alternatively, the 2D $e$-$h$ pairs are eliminated, if the transition rate of the 2D $e$-$h$ pairs with energies above $E_G$ to the 3D $e$-$h$ pairs owing to the phonon interaction is high, or if the rate of the Auger transitions involving the 3D $e$-$h$ pairs is high.

The ablation thresholds on well-annealed surfaces obtained by 540- and 600-nm laser pulses are approximately the same (Figs. 7 and 8), indicating that 2D and 3D $e$-$h$ pairs are equally effective in causing the ablation. Measurements of the temperature dependence similar to those for the $A$ and $S$ components resulted in the same conclusion.[34] It is likely that the densities of 2D and 3D $e$-$h$ pairs at the defects (vacancies) which initiate ablation are almost the same. We note that the values of the ablation threshold are remarkably scattered for excitation in range III. The result indicates that the substantial difference is between the nature of the excitation in ranges I and II and that in range III. We interpret the scattering as being due to the localized nature of the electronic excited states induced in range III, and inhomogeneous distribution of defects on surfaces. Because of the diffusion of the 2D and 3D $e$-$h$ pairs, the effects of the inhomogeneous defect distribution will be smeared out.

### E. Properties of laser- and $Ar^+$-damaged surfaces

The laser-induced emission of $Ga^0$ exhibits different features for laser- and $Ar^+$-damaged surfaces. Surfaces after laser damage do not show nearly any $A$ and $S$ components, but the ablation occurs at much lower laser fluences than on undamaged surfaces. On the other hand, both the $A$ and $S$ components are enhanced remarkably by $Ar^+$ bombardment, while the ablation threshold is not modified appreciably.

Bombardment with 500-eV $Ar^+$ produces the knock-on damage on the surface layers of a depth of a few monolayers. The damaged part includes the point defects and even amorphous structures. The stoichiometry may be changed slightly because of preferential sputtering.[30] It appears that the laser beams of subgap photon energies can excite the defects generated by $Ar^+$-bombardment and cause the $A$- and $S$-type emissions. The results that repeated irradiation with laser pulses reduces most of these components and makes the ablation threshold not much smaller than that before $Ar^+$ bombardment suggests that the $Ar^+$-induced damage is removed almost completely by laser.

It is known that the laser beams with a fluence above the ablation threshold produce a thick Ga-rich layer.[32] Thus, the low ablation threshold for laser-damaged surfaces may be ascribed to the enhancement of the optical-absorption coefficient due to formation of the Ga-rich layer. The laser ablation of the laser-damaged surfaces is considered to be governed by the heating rather than the

evolution of the vacancy cluster, as for the undamaged surfaces.

The present investigation indicates that the laser-induced particle emission for subgap photon energies and subthreshold fluences is enhanced by damage of the surfaces. The mode of enhancement of the emission yield reflects the mode of the surface damage to some extent: The physical damage induces the enhancements of the $A$ and $S$ components, while the stoichiometry change induces the change in the ablation threshold.

### F. The mechanism of laser-induced sputtering

In discussing the mechanism for multihole localization on a surface defect, we base our work on the following. First, the energy possessed by the localized electronic excited state is directly converted into the atomic energy, resulting in the particle emission. Unlike the Knotek-Feibelman process, the phenomena will be adiabatic, and the criterion for emission after electronic excitation is whether the APES of the excited state has a minimum or whether it is a decreasing function leading to particle emission. In some solids, such as alkali halides, an exciton (the singly excited state) has an instability leading to the emission.[16] Second, a localized hole is the source of bond weakening:[38] the more holes there are localized on a defect atom on the surface, the weaker the bond becomes. In some sense the negative-$U$ interaction suggested for defects in the bulk[24] is a manifestation of this phenomenon—the adiabatic potential energy is lower when two holes are localized than when one hole is localized. Since the negative-$U$ localization of two holes on a defect in bulk is a well-accepted concept,[39] we consider the negative-$U$ two-hole localization on defects on surfaces is the primary process for particle emission.

Now, the next question we have to answer is how multihole localization is induced under laser irradiation. Once two holes are localized on a defect under a dense $e$-$h$ plasma, the electrons are attracted by the Coulomb force of the holes. A defect with two localized holes, to which two electrons are bound, can be regarded as a doubly excited defect or two localized $e$-$h$ pairs on the defect. Because of the strong electron-lattice interaction inducing the negative $U$, we consider that the APES minimum for the doubly excited state is separated from the singly excited and ground state by a potential barrier; thus the doubly excited state forms a metastable state, having a long life.[40] Thus, we consider that the doubly excited state is further excited during a laser pulse, resulting in a multiply excited state. Since the doubly excited state, suggested by Wu,[22] induced by the Auger processes has a short lifetime, we consider that the two-hole state suggested by him cannot be the source of the multiple excitation.

A typical APES describing such a negative-$U$ state and multiply excited states is shown in Fig. 12, where curve $E_1$ in the figure is a singly excited state and $E_2$ is the doubly excited negative-$U$ state. Because of strong lattice relaxation, the energy of electronic transition will not change appreciably as the multiplicity increases, as often observed in an isolated small molecule. A schematic

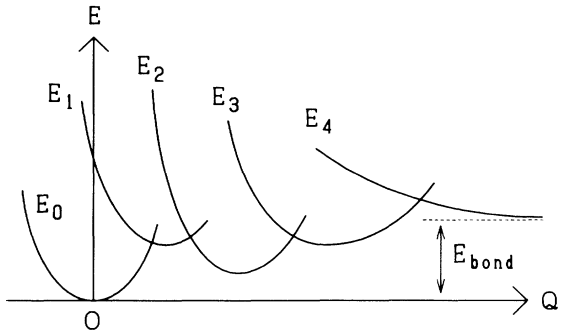


FIG. 12. Schematic adiabatic potential-energy surfaces (APES's) explaining a cascade-excitation mechanism of laser-induced particle emission. Multiple excitation of a defect site, from a ground state $E_0$ via metastable states $E_1$–$E_3$ to an unstable state $E_4$, leads to particle emission. $E_{\text{bond}}$ denotes the energy needed to emit an atom by this mechanism. The lower minimum of state $E_2$ compared with state $E_1$ shows the negative-$U$ effect.

APES for the negative-$U$ defect after the third excitation is shown by $E_3$ of Fig. 12. The doubly excited state will be further excited to $E_3$ during its lifetime. Such cascade excitation will finally lead to bond breaking, if the APES for a certain multiply excited state ($E_4$ in Fig. 12) is antibonding.[41] We presume that such a relaxed multiply excited state is feasible on surfaces because of the high flexibility of the lattice, although generation of such highly excited states will cost much energy in the bulk. If the lifetime of the metastable states is longer than the pulse width, the probability of the atoms to be emitted will show a power function of the fluence, as is indeed observed experimentally, and here the number of the index will represent the same index as the multiplicity of the cascade needed for the emission.

For photons that are capable of exciting only defects, the above pictures should be slightly modified. Here the successive double excitation of a defect should produce the negative-$U$ state, which serves as the source of further multiple excitation. Since the experimental values of the threshold laser fluence for photons of photon-energy ranges II and III do not differ too much for the $A$ and $S$ components, the cascade excitation should play a substantial role for these components. On the other hand, absence of fluctuation of the ablation threshold for photons with energies of ranges I and II, in spite of a large fluctuation for those of range III, suggests that the initial localization plays a role for laser ablation.

Recently, Ong *et al.*[42] have calculated the energies needed to remove a $Ga^0$ atom that neighbors various types of defects on surfaces: They calculated differences in the energy of a GaP cluster with a surface defect before and after removal of a $Ga^0$ atom. According to their results, the energy to remove a $Ga^0$ atom from an adatom is smaller than that to remove it from a step site. Thus, it appears that the higher multiplicity is needed to remove a more strongly bonded defect atom. It is not yet clear that the energy calculated by Ong *et al.* corresponds to $E_{\text{bond}}$ shown in Fig. 12. If one assumes that the thermal

ejection occurs through the same electronic state as the ejection after multiple excitation, we may presume that a higher multiplicity is needed to eject a more strongly bonded $Ga^0$ atom, in view of Fig. 12.

The model described above is still tentative. The behaviors of an $e$-$h$ plasma in the presence of defects with a highly deformable lattice have not been explored. The possibility of trapping of additional $e$-$h$ pairs to a multiply excited state cannot be excluded. The essence of the model is that a multiply excited state of a defect atom on the surface, accomplished with substantial lattice relaxation, is induced, and the bond weakened by the multihole localization is broken by virtue of the electronic excitation energy.

## V. CONCLUSIONS

In this paper we have shown the features of defect-initiated particle emission induced by irradiation with laser pulses of three photon-energy ranges: I, sufficient to generate band-to-band excitation; II, insufficient to produce band-to-band transitions, but sufficient to produce transitions of valence electrons to unoccupied surface states; and III, insufficient to induce either of these transitions, but possibly capable of exciting surface defects. It is found that the features of particle emission revealed through measurements of the $Y$-$\phi$ and $Y$-$n$ relations are strikingly dependent on the photon-energy range. Although the photons of energy range I induce the laser ablation, they are incapable of inducing the particle emission initiated by defects on surfaces, which occur below the ablation threshold. The photons of energy range II induce the ablation nearly at the same laser fluence as those of range I, and also induce the defect-initiated particle emission below the ablation threshold. The photons of energy range III also induce the defect-initiated particle emission, as well as the ablation, but the ablation threshold for photons of this energy range is scattered, indicating the local character of the transitions induced. The defects initiating particle emission, below laser ablation threshold, are ascribed to adatom- and kink-type defects on surfaces. It is suggested that laser ablation is initiated by vacancies on surfaces. The interpreation of the results is based on the presumption that photons of ranges I, II, and III produce the 3D bulk $e$-$h$ pairs, 2D surface $e$-$h$ pairs, and defect excitation, respectively.

Because of the nonlinear character of the $Y$-$\phi$ relations, which are fitted to the power functions, emission is ascribed to multiple excitation of, or multiple electron-hole localization on, the surface defects. It is shown that the power index of the $Y$-$\phi$ relation depends on the type of defect and on the processes that produce the defects. A mechanism of localization by virtue of strong electron-lattice coupling of defects on surfaces due to their flexible structures is suggested.

The present investigation gives insight into the defects on surfaces of relatively small concentration ($10^{-5}$ ML). In particular, the results indicate that the measurements of particle emission serve as a powerful tool for characterization of defects on surfaces. Although scanning tunneling microscopy (STM) is a useful tool for observing defects, the present technique gives complementary information, namely the quantitative values of the concentration of specific types of defects on surfaces. Furthermore, the present investigation shows that defects on surfaces can be removed by repeated irradiation with laser pulses below the ablation threshold. Further studies of defects on surfaces by means of STM and laser-induced particle emission would be of use.

## ACKNOWLEDGMENTS

This work was supported by a Grant-in-Aid from the Japanese Ministry of Education, Science and Culture. The authors would like to thank Professor R. F. Haglund, Jr., Professor C. K. Ong, Professor H. Sumi, and Professor J. Singh for stimulating discussions. They would also like to express their gratitude to H. Matsuoka for assistance in constructing a part of the experimental apparatus, and to T. Gotoh for technical assistance with SEM and EPMA.

*Present address: The Institute for Solid State Physics, The University of Tokyo, 7-22-1 Roppongi, Minato-ku, Tokyo 106, Japan.

[1]M. Von Allmen, *Laser-Beam Interactions with Materials* (Springer-Verlag, Berlin, 1987).

[2]T. J. Chuang, in *Interfaces Under Laser Irradiation,* edited by L. D. Laude, D. Bauerle, and M. Wautelet (Nijhoff, Dordrecht, The Netherlands, 1987), p. 235.

[3]J. Reif, Opt. Eng. **28**, 1122 (1989).

[4]A. A. Marenkov and A. M. Prokhorov, Usp. Fiz. Nauk **148**, 179 (1986) [Sov. Phys.—Usp. **29**, 104 (1986)].

[5]N. Itoh, Nucl. Instrum. Methods **132**, 201 (1976); P. D. Townsend and F. Lama, in *Desorption Induced by Electronic Transitions,* edited by N. H. Tolk, M. M. Traum, J. C. Tully, and T. E. Madey (Springer-Verlag, Berlin, 1983), p. 220; R. T. Williams, and K. S. Song, J. Phys. Chem. Solids **51**, 679 (1990).

[6]H. Kanzaki and T. Mori, Phys. Rev. B **29**, 3573 (1984).

[7]J. Schou, Nucl. Instrum. Methods B **27**, 188 (1987).

[8]T. Nakayama, Surf. Sci. **133**, 101 (1983).

[9]T. Nakayama, H. Ichikawa, and N. Itoh, Surf. Sci. **123**, L693 (1982); T. Nakayama and N. Itoh, in *Desorption Induced by Electronic Transitions,* edited by W. Brenig and D. Menzel (Springer-Verlag, Berlin, 1985), p. 237; Y. Kumazaki, Y. Nakai, and N. Itoh, Surf. Sci. **184**, L445 (1987); Phys. Rev. Lett. **59**, 2883 (1987);

[10]A. Namiki, T. Kawai, and K. Ichige, Surf. Sci. **166**, 129 (1986); K. Ichige, Y. Matsumoto, and A. Namiki, Nucl. Instrum. Methods B **33**, 820 (1988).

[11]A. Namiki, K. Watanabe, H. Fukano, S. Nishigaki, and T. Noda, Surf. Sci. **128**, L243 (1983); A. Namiki, H. Fukano, T. Kawai, Y. Yasuda, and T. Nakamura, J. Phys. Soc. Jpn. **54**, 3162 (1985); A. Namiki, K. Watanabe, H. Fukano, S. Nishigaki, and T. Noda, J. Appl. Phys. **54**, 3443 (1983); A. Namiki, T. Kawai, Y. Yasuda, and T. Nakamura, Jpn. J. Appl. Phys. **24**, 270 (1985).

[12]R. W. Dreyfus, R. Kelly, and R. E. Walkup, Appl. Phys. Lett. **49**, 1478 (1986); R. W. Dreyfus, R. E. Walkup, and R. Kelly, Radiat. Eff. **99**, 199 (1986).

[13]J. E. Rothenberg and R. Kelly, Nucl. Instrum. Methods B **1**, 291 (1984); R. Kelly and J. E. Rothenberg, *ibid.* **7/8**, 755 (1985); R. Kelly, J. J. Coumo, P. A. Leary, J. E. Rothenberg, B. E. Braren, and C. F. Aliotta, *ibid.* **9**, 329 (1985); R. W. Dreyfus, F. A. McDonald, and R. J. von Gutfeld, J. Vac. Sci. Technol. B **5**, 1521 (1987).

[14]D. Menzel and R. Gomer, J. Chem. Phys. **41**, 331 (1964).

[15]P. Readhead, Can. J. Phys. **42**, 886 (1964).

[16]N. Itoh and K. Tanimura, J. Phys. Chem. Solids **51**, 717 (1990).

[17]N. Itoh, Cryst. Lattice Defects Amorph. Mater. **12**, 103 (1985).

[18]In these solids, the two-photon absorption under laser irradiation, which also causes low-intensity band-to-band transitions, can induce particle emission and, consequently, surface damage. See E. Matthias and T. A. Green, in *Desorption Induced by Electronic Transitions,* edited by G. Betz and P. Varga (Springer-Verlag, Berlin, 1990), p. 112; H. Cronberg, W. Muydermann, H. B. Nielsen, E. Matthias, and N. H. Tolk, *ibid.*, p. 157.

[19]M. L. Knotek and P. J. Feibelman, Phys. Rev. Lett. **40**, 964 (1978).

[20]N. Itoh, Nucl. Instrum. Methods B **27**, 155 (1987).

[21]K. Hattori, Y. Nakai, and N. Itoh, Surf. Sci. **227**, L115 (1990).

[22]Z. Wu, in *Desorption Induced by Electronic Transitions* (Ref. 18), p. 163.

[23]N. Itoh and T. Nakayama, Phys. Lett. A **92**, 471 (1982); N. Itoh, T. Nakayama, and T. A. Tombrello, *ibid.* **108**, 480 (1985).

[24]P. W. Anderson, Phys. Rev. Lett. **34**, 953 (1975).

[25]H. Sumi, Surf. Sci. **248**, 382 (1991).

[26]K. Hattori, A. Okano, Y. Nakai, N. Itoh, and R. F. Haglund, Jr., J. Phys.: Condens. Matter **3**, 7001 (1991).

[27]F. Cerrina, A. Bommannavar, R. A. Benbow, and Z. Hurych, Phys. Rev. B **31**, 8314 (1984); D. Straub, M. Skibowski, and F. J. Himpsel, J. Vac. Sci. Technol. A **3**, 1484 (1985); D. Straub, V. Dose, and W. Altman, Surf. Sci. **133**, 9 (1983).

[28]F. Manghi, C. M. Bertoni, C. Calandra, and E. Molinari, Phys. Rev. B **24**, 6029 (1981).

[29]The gap between the top of the valence band ($\bar{\Gamma}$ point) and the bottom of the conduction band in GaP at room temperature is 2.26 eV, while the $\bar{\Gamma}$ point of the unoccupied surface state has been shown to exist 0.3 eV below the bottom of the conduction band through inverse-photoemission experiments. Theoretical calculation indicates, however, that the bottom of the unoccupied surface state is at the $\bar{X}$ point and is 1.53 eV above the top of the valence band. Therefore, we used 540 nm (2.30 eV) for photon-energy range I, 600 nm (2.07 eV) for range II, and 870 nm (1.43 eV) and 920 nm (1.34 eV) for range III.

[30]A. J. Van Bommel and J. E. Crombeen, Surf. Sci. **93**, 383 (1980).

[31]G. S. Hurst, M. G. Payne, S. D. Kramer, and J. P. Young, Rev. Mod. Phys. **51**, 767 (1979); T. Yamamoto, K. Hattori, Y. Nakai, and N. Itoh, Radiat. Eff. Defects Solids **109**, 213 (1989).

[32]C. L. Anderson, in *Laser and Electron-Beam Interactions with Solids,* edited by B. R. Appleton and G. K. Celler (North-Holland, New York, 1982), p. 653; M. Okigawa, T. Nakayama, K. Morita, and N. Itoh, Appl. Phys. Lett. **43**, 1054 (1983), and references therein.

[33]The difference from the value of $\phi_D$ for Fig. 3 is within experimental error.

[34]A. Okano, K. Hattori, Y. Nakai, and N. Itoh, Surf. Sci. **258**, L671 (1991).

[35]We consider that the atoms bonded less strongly than those of the perfect surface sites can initiate emission, and we refer to these atoms as defect atoms. For instance, a P vacancy on the the GaP (110) surface includes three defect atoms.

[36]Y. Nakai, K. Hattori, A. Okano, N. Itoh, and R. F. Haglund, Jr., Nucl. Instrum. Methods B **58**, 452 (1991).

[37]A. Okano, K. Hattori, Y. Nakai, and N. Itoh, Appl. Phys. Lett. (to be published).

[38]Weakening bonds of solids by generation of high-density unlocalized holes has been discussed by Van Vechten *et al.* [J. A. Van Vechten, R. Tsu, and F. W. Saris, Phys. Lett. A **74**, 422 (1979)]. An unlocalized hole makes only a partial contribution to the weakening of the bonds in solids, proportional to the average concentration. A localized hole at a specific site will directly weaken the bond around the localized sites and, hence, will be more efficient.

[39]G. D. Watkins, in *Festkörperprobleme,* edited by P. Grosse (Pergamon/Viewig, Braunschweig, Germany, 1984), Vol. 24, p. 163.

[40]G. D. Watkins, Mater. Sci. Forum **38-41**, 39 (1989).

[41]One can visualize the APES curves of Fig. 12 in the following way. Suppose a Ga adatom singly bonded to a P atom on the surface is placed under a dense electron-hole plasma on the surface. The first trapped hole will probably be located on the bond connecting the adatom, and $E_1$ represents the APES with the defect with the hole to which an electron is bound. The energy minimum will occur at the bond length that is longer than the ground state. The next hole will be located more in the bonds connecting the P atom underneath to the surrounding Ga atoms on the surface top layer. Thus, the minimum for $E_2$ involves the relaxation on the atoms on the surface top layer as well as the bond for the adatom. Additional excitation will induce further relaxation and, finally, as the number of the hole increases, the adatom bond will become unstable.

[42]C. K. Ong, G. S. Khoo, N. Itoh, and K. Hattori, Surf. Sci. **259**, L787 (1991).